RSC Advances

ROYAL SOCIETY OF CHEMISTRY

www.rsc.org/advances

Journal Name

ARTICLE

Multicompartment Micelles Based on Hierarchical Co-Assembly of PCL-*b*-PEG and PCL-*b*-P4VP Diblock Copolymers

Received 00th January 20xx,
Accepted 00th January 20xx

DOI: 10.1039/x0xx00000x

www.rsc.org/

Xue Liu,[a] Yu Hou,[a] Xiuping Tang,[a] Qiuhua Wu,[a] Chenglin Wu,[b] Jie Yi[a] and Guolin Zhang*[a]

Multicompartment micelles are prepared via the hierarchical co-Assembly of two diblock copolymers, poly(ε-caprolactone)-*b*-poly(ethylene glycol) (PCL-*b*-PEG) and poly(ε-caprolactone)-*b*-poly(4-vinylpyridine) (PCL-*b*-P4VP) in aqueous solution. These two polymers first assemble into mixed shell micelles through hydrophobic interaction among PCL chains. PCL chains form the micellar core, while PEG and P4VP chains form the micellar shell. Regulating the pH value above the pKa of P4VP can induce hydrophobic phase-segregated P4VP patches forming on the surface of mixed shell micelles. When hydrophilic PEG chains cannot stabilize theses micelles with hydrophobic patches, they will furthermore assemble as the subunits into MMs with different morphologies. These MMs can be revealed by transmission electron microscopy through P4VP chains positive staining.

Introduction

Design and preparation of multifunctional nanomaterials is one of the most important themes of recent research. Self-assembly provides a powerful platform for preparing nanomaterials with complicated structure and novel function.[1-2] In the field of polymeric material, through self-assembly of amphiphilic diblock copolymers, versatile micelles are constructed, including spheres, cylinders, rods, worms, lamellae, or vesicles.[3-4] Recently, more attention focuses on their potential application in a variety of fields, such as supports for catalytic devices, drug delivery carriers, separation technology, lithographic templates and so on.[5-8] However, more advanced function demands a more complicated structure combining various compartments to cooperate, which gave rise to multicompartment micelles (MMs).

This concept of MMs drew inspiration from organized biological systems, such as perfectly functioning proteins, which possess complex quaternary structures composed of several subunits combining diverse properties, environments, and functions. A simple natural example for such systems is serum albumin, which owns several independent "binding pockets" of different quality, and enables selective uptake and release of different "transport goods" in blood, such as poorly water-soluble compounds.[9] These subunits are first constructed through the precise folding of peptides, and then the assembled subunits further proceed the hierarchical assembly into the final multi-subunit protein structure.

Inspired from these natural structure, MMs are also constructed by multi-level assembly, taking multi-block copolymers or multiple copolymers as the basic blocking units.[10] The assembling process in solution can be driven by various noncovalent interactions, such as hydrophobic interactions, electrostatic interactions, hydrogen bonding and so on. However, most of the time, with increasing size and complexity of the subunits, the kinetic obstacles become significant and trapping of metastable species can occur, preventing well-defined solution hierarchies of low polydispersity on an appropriate timescale.[11-12] Müller and his coworkers carried out a series of systematical studies about the MMs constructed with simple linear ABC triblock terpolymers through the directed step-wise hierarchical self-assembling method.[13-16] The intermediate pre-assembly of subunits without precedent structural control was fabricated in the first step. Homogeneous MMs were constructed via solvent-regulated hierarchical self-assembly of the intermediate pre-assembled subunits. Compared with the previous one-step dissolution (or direct dialysis) method, this directed self-assembly led to a step-wise reduction of the degree of conformational freedom and dynamics and avoided undesirable kinetic obstacles during the structure build-up.

Müller's method to prepare MMs through directed step-wise self-assembly using pre-assembled subunits is very enlightening. However, there exit some problems for the basic building blocks--triblock terpolymers, which usually involve in numerous and complicated synthetic procedures. In addition, the structural adjustment of the MMs assembled by triblock terpolymers is realized through regulating the polymerization degree of each block, which results in more synthetic tasks. The nanostructure assembled by triblock terpolymers can also be prepared through direct mixing of two kinds of diblock copolymers, which is also called co-assembly strategies.[17] The materials constructed via co-assembly strategies have shown potential as smart carriers in drug delivery processes.[18-20] Such concepts have also been employed for the preparation of MMs.[21-24] For example, micelles with a mixed shell can be assembled by ABC triblock terpolymers. The insoluble B block

[a]*Liaoning Province Key Laboratory for Green Synthesis and Preparative Chemistry of Advanced Materials, College of Chemistry, Liaoning University, Shenyang, 110036, (P. R. China), Fax: (+86) 24-6220-2380, E-mail: glzhang@lnu.edu.cn*
[b]*School of Pharmaceutical and Chemical Engineering, Taizhou University, Taizhou, 317000, (P. R. China)*

forms the micellar core, and the soluble A and C blocks extent into the solution to form the mixed shell. Such mixed shell micelle can also be constructed by mixing AB and BC amphiphilic diblock copolymers, and the assembling process is shown in Scheme 1. Compared with the MMs constructed by triblock terpolymers, the composition, structure and property of the MMs can be conveniently designed and adjusted only through changing the composing proportion of these two diblock copolymers. Therefore, in this research, we selected two amphiphilic diblock copolymers as the basic building blocks to construct the subunit of MMs.

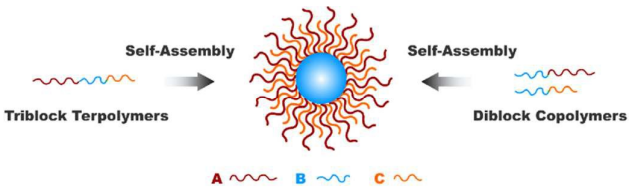

Scheme 1. Schematic representation of the micelle with a mixed shell assembled by one triblock terpolymer or two diblock copolymers. A and C: soluble blocks; B: insoluble block.

A pH-responsive mixed shell polymeric micelles (MSPMs) were prepared as the subunit to construct MMs through the co-self-assembly of two amphiphilic diblock copolymers: poly(ε-caprolactone)-*b*-poly(ethylene oxide) (PCL-*b*-PEG) and poly(ε-caprolactone)-*b*-poly(4-vinylpyridine) (PCL-*b*-P4VP) in solution. Hydrophobic PCL chains aggregated and formed the core of the MSPMs, while the hydrophilic PEG chains and P4VP chains spreading around the surface of the MSPMs formed the mixed shell. P4VP is a pH dependent polymer with a pKa at ca. 4.5~4.7.[25] Below the pKa, P4VP is soluble as a weak cationic polymer due to the protonation of the pyridine groups. Above the pKa, due to the deprotonating effect, P4VP turns hydrophobic. Therefore, when regulating the pH value in solution above the pKa of P4VP, phase transition from hydrophilicity to hydrophobicity happened to P4VP. Accordingly, MSPMs evolved into MMs with various structures and morphologies. The structure and morphology of the MMs depend on the composition of the MSPMs. When P4VP content is less, PEG chains can stabilize the micelles. Hydrophobic P4VP chains collapse on the surface of the micelles and form separated patches, and MSPMs transform into core-patch-corona micelles (CPCMs). Further increasing the content of P4VP chains on the surface of MSPMs, separated and hydrophobic P4VP patches will aggregate into continuous phase. If there are enough hydrophilic PEG chains, 'inverse hamburger' micelles can be formed and stable in solution without aggregation. When PEG chains cannot stabilize the micelles anymore, MSPMs will transform into transient and unstable Janus-type micelles, which will further assemble into MMs with novel morphologies, including 'hamburger' micelles, 'football' micelles and 'vesicle-like' micelles. The morphology types depend on the assembling number of the participant subunits. The structure and morphology of the MMs could be observed clearly through staining the TEM (transmission electron microscope) samples with uranyl acetate.

Material

Methoxy poly(ethylene glycol) (mPEG) (M_w=2000, polydispersity index=1.05, Fluka) was dried in vacuum for 24 hours prior to use. 2-Hydroxyethyl 2-bromoisobutyrate (HEBIB) and Tris[2-(dimethylamino)-ethyl]amine (Me_6TREN) were synthesized according to the previous reports.[26, 27] CuCl (97%, Sigma-Aldrich) and 4-vinylpyridine (4VP, 96%, Alfa Aesar) were purified before use.[28, 29] Stannous octoate ($Sn(Oct)_2$, 96%, Alfa Aesar), ε-caprolactone (CL, 99%, Alfa Aesar) and uranyl acetate (Beijing Zhongjingkeyi Technology Co., Ltd) was used without further purification. All solvents were dried and redistilled before use.

Experimental

Synthesis of the Diblock Copolymers

Synthesis of PEG-*b*-PCL. Synthesis of PEG-*b*-PCL was illustrated in Figure 1A. PEG-*b*-PCL was synthesized by ring-opening polymerization (ROP) of CL using PEG-OH as the initiator and $Sn(Oct)_2$ as the catalyst in toluene solution, referring to the method of Shi et al.[30] Briefly, PEG-OH (2 g, 1 mmol), CL (4.0 g, 35 mmol), and $Sn(Oct)_2$ (0.19 g, 0.48 mmol) were added into the reaction flask and then toluene (20 mL) was added. After freeze-degas-thaw cycles, polymerization was performed at 120 °C for 12 hours. Then the mixture was diluted with dichloromethane and then precipitated into excess diethyl ether. The precipitate was dried under vacuum.

Synthesis of PCL-*b*-P4VP. Referring to the method of Shi et al,[30] PCL-Br macroinitiator was synthesized by ROP of CL using HEBIB as the initiator and $Sn(Oct)_2$ as the catalyst in toluene solution. Briefly, HEBIB (0.42 g, 2 mmol), CL (13.6 g, 120 mmol), and $Sn(Oct)_2$ (0.96 g, 2.4 mmol) were added into the reaction flask and then 26 mL toluene was added. Polymerization was conducted at 110 °C for 12 hours after freeze-degas-thaw cycles. Dichloromethane was added to dilute the as-prepared mixture, which was further precipitated into excess diethyl ether. PCL-*b*-P4VP was synthesized by atom transfer radical polymerization (ATRP) using PCL-Br as the initiator and CuCl/Me_6Tren as the catalyst in butanone/ isopropanol mixed solvent. Briefly, PCL-Br (1.0 g, 0.1 mmol), CuCl (0.012 g, 0.1 mmol), Me_6TREN (0.046 g, 0.2 mmol), and 4VP (0.5 g, 4.8 mmol) were added into the reaction flask and then butanone/2-propanol (7:3 *v*:*v*, 8 mL) was added. After freeze-degas-thaw cycles, polymerization was performed at 45 °C for 4 hours. The mixture was purified by dialyzing against water in a dialysis bag with a molecular cutoff of 7 KD, and PCL-*b*-P4VP was obtained after lyophilization.

Preparation of the Subunits. Subunits preparation was realized according to a traditional preparation method through self-assembly of amphiphilic block copolymers.[30] Block copolymers PEG-*b*-PCL and PCL-*b*-P4VP were first dissolved in

THF to make the polymer solution with a concentration of 1.0 mg mL^{-1}, respectively. For preparing a specific micelle, a quantitative of PEG-*b*-PCL and PCL-*b*-P4VP solutions was mixed together first. For example, MSPMs (1/1) were prepared through mixing equal volume of PEG-*b*-PCL and PCL-*b*-P4VP solutions. Subsequently, a given amount of acid water (pH=2.0) was added dropwise into polymer solution under vigorous stirring until opalescence appeared, indicating the formation of micelles. The solution was stirred overnight and then dialyzed against acid water (pH=2.0) in a dialysis bag (molecular weight cut off: 12~14 KD) to remove THF. MSPMs with the other compositions were prepared in the same way, including MSPM (3/1), MSPM (1/4) and MSPM (3/17).

Preparation of Multicompartment Micelles. The as-prepared subunits based on MSPMs were dialyzed against neutral aqueous solution in a dialysis bag (molecular weight cut off: 12~14 KD). Phase transition from hydrophilicity to hydrophobicity happened to P4VP, and MSPMs transformed to MMs. Regulating the composition (the weight ration of PCL-*b*-PEG to PCL-*b*-P4VP) of MSPM, MMs with various structures were formed through the self-assembly of MSPMs.

Characterizations. ^{1}H nuclear magnetic resonance (^{1}H NMR) spectra were recorded on a Varian UNITY-plus 400 M NMR spectrometer at room temperature with $CDCl_3$, using tetramethylsilane (TMS) as a reference. Relative molecular weights and molecular weight distributions of block copolymers were measured by gel permeation chromatography (GPC) at 35 °C with a Waters 1525 chromatograph equipped with a Waters 2414 refractive index detector. GPC measurements were carried out using THF as eluents with a flow rate of 1.0 mL min^{-1}, respectively. Polystyrene (PS) standards were used for calibration. Dynamic light scattering (DLS) and static light scattering (SLS) measurements were performed on a laser light scattering spectrometer (BI-200SM) equipped with a digital correlator (BI-10000AT) and a laser source of 532 nm. Filtering solutions through a 0.45 mm Millipore filter into a clean scintillation vial allowed us to obtain the samples for characterization. TEM measurements were performed with a commercial Philips T20ST electron microscope at an acceleration voltage of 200 kV. To prepare the TEM samples, a small drop of the solutions was deposited onto the carbon-coated copper electron microscopy (EM) grid in the thermo-stated container and then dried under room temperature and atmospheric pressure. 2% uranyl acetate aqueous solution was prepared to stain the TEM samples.

Results and discussion

Synthesis of Diblock Copolymers. The block copolymer PEG-*b*-PCL was synthesized by ROP of CL, using PEG-OH as the macroinitiator. The block copolymer PCL-*b*-P4VP was synthesized by a combination of ROP and ATRP. First, HEBIB was used to initiate the ROP of CL to obtain the macroinitiator PCL-Br, which was applied to initiate the ATRP of 4VP to get the block copolymer PCL-*b*-P4VP. Figure 1 shows the synthesis steps of PEG-*b*-PCL (Figure 1A) and PCL-*b*-P4VP (Figure 1B), as well as the ^{1}H NMR spectra of HEBIB (Figure 1C), PCL-Br (Figure 1D), PEG-*b*-PCL (Figure 1E) and PCL-*b*-P4VP (Figure 1F) in $CDCl_3$. For HEBIB, the resonance band observed in the regions of 3.87 (C-a) ppm is attributed to the methylene protons close to the hydroxyl group. While the resonance band observed in the regions of 4.30 (C-b) ppm is attributed to the methylene protons close to the ester group. The band at 1.95 (C-c) ppm is attributed to tert-butyl protons. The number-average molecular weight (M_n) of PCL can be calculated according to the relative intensities of the methylene protons (D-b, E-b) in the backbone of PCL, compared to that of the tert-butyl protons (D-a) of HEBIB and the methylene protons in the backbone of PEG (E-a). The M_n of P4VP can be calculated according to the relative intensities of the pendent pyridine protons of P4VP compared to that of the methylene protons in the backbone of PCL. The M_n and polydispersity index (PDI) of PCL-Br, PEG-*b*-PCL and PCL-*b*-P4VP from GPC and ^{1}H NMR tests are listed in Table 1. Based on the relative intensities of the characteristic groups in the ^{1}H NMR, these two diblock copolymers were denoted as PCL_{80}-*b*-PEG_{45} and PCL_{100}-*b*-$P4VP_{87}$, respectively.

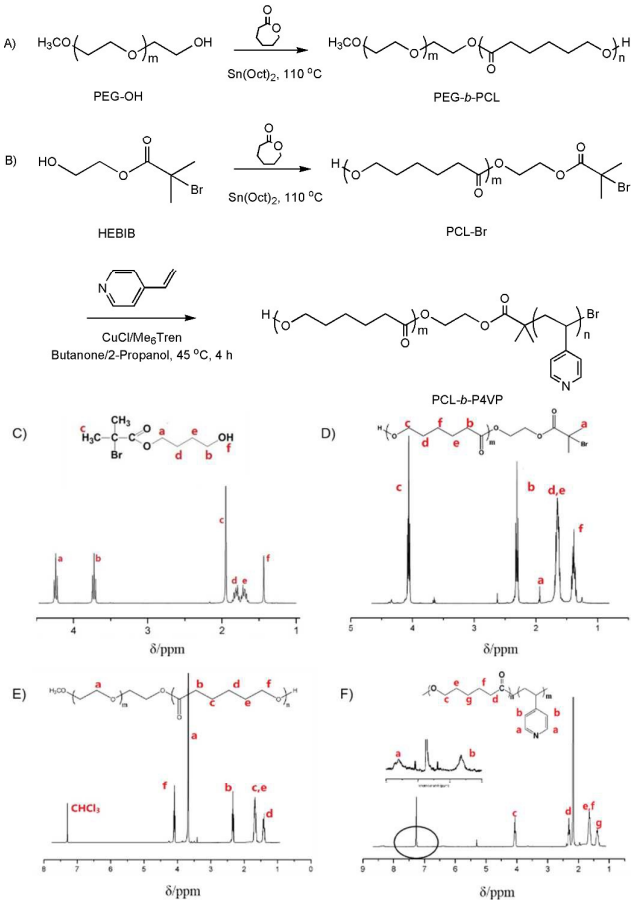

Figure 1. A) The synthesis of PEG-*b*-PCL. B) The synthesis of PCL-*b*-P4VP. C) The ^{1}H NMR spectra of HEBIB. D) The ^{1}H NMR spectra of PCL-Br. E) The ^{1}H NMR spectra of PEG-*b*-PCL. F) The ^{1}H NMR spectra of PCL-*b*-P4VP.

Table 1. The number-average molecular weight (M_n) and polydispersity index (PDI) of PCL-Br, PEG-*b*-PCL and PCL-*b*-P4VP.

	M_n from ^{1}H NMR ($\times 10^4$)	M_n from GPC ($\times 10^4$)	PDI
PCL-Br	1.14	0.99	1.19
PEG-*b*-PCL	1.11	1.59	1.11
PCL-*b*-P4VP	2.05	1.92	1.08

Preparation of Subunits. Amphiphilic diblock copolymers can self-assemble into core-shell micelles in solution. In acid aqueous solution (pH=2.0, below the pKa of P4VP), due to the protonation of pyridine groups, P4VP chains show hydrophilic, and PCL-*b*-P4VP diblock copolymers is amphiphilic. Therefore, when a mixture of two amphiphilic diblock copolymers including PEG-*b*-PCL and PCL-*b*-P4VP was placed in such acid aqueous solution, MSPMs can be formed. Hydrophobic PCL chains formed the common micellar core, and hydrophilic PEG and P4VP chains stretched around the micellar core forming the mixed shell. The schematic MSPMs formed by PEG-*b*-PCL and PCL-*b*-P4VP are shown in Scheme 2.

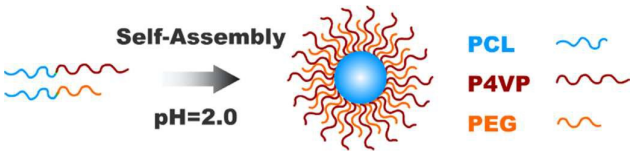

Scheme 2. Schematic representation of the structure of the as-prepared subunits based on the mixed shell polymeric micelles (MSPMs).

During the preparing process of the MSPMs, PEG-*b*-PCL and PCL-*b*-P4VP were dissolved in the THF solution with the same concentration (1 mg mL^{-1}). Therefore, the MSPMs with different compositions (PEG-*b*-PCL/PCL-*b*-P4VP=3/1, 1/1, 1/4 and 3/17, mass ratio) were prepared through directly mixing these two diblock copolymers THF solutions with various volume ratios before replacing the co-solvent into the selective solvent, and the final achieved MSPMs with corresponding mass ratios of PEG-*b*-PCL to PCL-*b*-P4VP. A similar method had been applied to confirm the formation of the MSPMs instead of a simple mixture of PEG-*b*-PCL micelles and PCL-*b*-P4VP micelles. [31] PCL-*b*-P4VP micelles would aggregate and precipitate when P4VP chains turn hydrophobic in alkaline solution, while MSPMs can keep stable with the protection of hydrophilic PEG chains. There was no precipitation appearing in alkaline MSPMs solution, which can effectively confirm that MSPMs have been formed.

DLS and SLS tests were applied to determine the morphological parameter of these subunits. Figure 2A shows the plot of the translational diffusion coefficient (D) versus q^2 of the MSPMs with four compositions. From the fitted line, the translational diffusion coefficient D^0 were calculated by extrapolating q^2 to 0 at a polymer concentration of 1.0 mg mL^{-1}. The translational diffusion coefficient D of the micelles are almost constants, which suggests the MSPMs are spherical. The hydrodynamic diameter distribution $f(D_h)$ of the MSPMs is shown in Figure 2B (scattering angle=90 °), which suggest that the D_h of the MSPMs is very narrowly distributed. The average hydrodynamic radius (R_h) according to Stokes-Einstein equation, radius of gyration (R_g) and R_g/R_h value are listed in Table 2. Along with the increase of the relative content of PCL-*b*-P4VP in the MSPMs, it should be pointed out that the D_h of the MSPMs has an increase from 90.8 to 121.7 nm. The hydrophobic PCL chain length of PCL_{100}-*b*-$P4VP_{87}$ is longer than that of PCL_{80}-*b*-PEG_{45}, which enlarged the grain diameter of the final MSPMs. It is well known that the R_g/R_h value reflects the morphology or conformation of polymer chains or the density distribution of particles in solution. [32] Compared with the uniform sphere ($R_g/R_h \approx 0.775$), the R_g/R_h of the MSPMs is a little larger, which suggests the structure of the MSPMs is relatively incompact. [33] Moreover, from MSPMs (3/1) to MSPMs (3/17), the R_g/R_h value increased from 0.813 to 0.953 and the structure of the MSPMs turned more and more incompact. We observed the morphology of the as-prepared subunits, and MSPMs (3/17) were chosen as the monitoring object (Figure 3). The micellar size observed in the TEM image is similar than that from the DLS results, which is ca. 100 nm. However, the TEM images present the samples under dried state, so the resulted sizes are less than those in solution. From the TEM image, we can see that, P4VP chains are stained by uranyl acetate and show a higher contrast. There exists a little phase-separation among PEG and P4VP chains on the surface of the subunits, which can be owe to the compatibility of two polymers. P4VP is hydrophilic in this situation, and therefore such phase-separation cannot result in an aggregation.

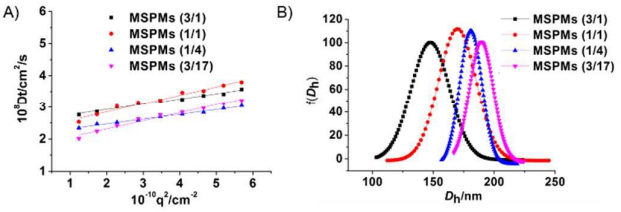

Figure 2. A) Angular dependence of the translational diffusion coefficient D_t and B) hydrodynamic diameter distribution f(D_h) of MSPMs with four compositions of PEG-*b*-PCL/PCL-*b*-P4VP (pH=2.0, scattering angle=90 °).

Table 2. The R_g, R_h and R_g/R_h of the MSPMs with four compositions of PEG-*b*-PCL/PCL-*b*-P4VP (pH=2.0).

MSPMs (PEG-*b*-PCL/PCL-*b*-P4VP)	R_g/nm	R_h ‡/nm	R_g/R_h
MSPMs (3/1)	73.9	90.8	0.813
MSPMs (1/1)	95.5	107.1	0.892
MSPMs (1/4)	109.9	115.7	0.949
MSPMs (3/17)	116.0	121.7	0.953

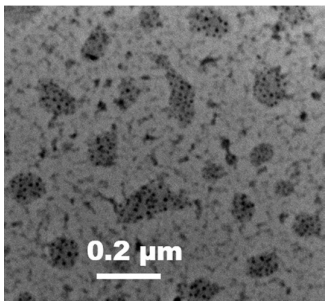

Figure 3. TEM image of the subunit composed of PEG-*b*-PCL/PCL-*b*-P4VP (3/17) stained by uranyl acetate (pH=2.0).

Preparation of Multicompartment Micelles. MMs were prepared through dialyzing MSPMs in neutral aqueous solution (pH=7.0). In this pH situation, deprotonating effect happened to P4VP, and P4VP chains turned hydrophobic. At the same time, the phase transition from hydrophilicity to hydrophobicity of P4VP chains induced the structure variation of the subunits. The hydrophobic and collapsed P4VP chains formed a new hierarchy, and the core-shell structure of MSPMs transformed into MMs with various structures. Through controlling the feed ration of two diblock copolymers during the preparation process of the subunits, the structure and morphology of the as-constructed MMs can be adjusted. The forming process of the MMs with various morphologies is presented in Scheme 3. Along with the increase of the hydrophobic P4VP section and the decrease of the exterior hydrophilic PEG chains around the micelles, the surface of the subunits showed more and more hydrophobic accordingly. When the amount of hydrophilic PEG chains are sufficient to stabilize the micelles, scattered hydrophobic P4VP patches can spread around the surface and CPCMs come into being first (Scheme 3-2). Further increasing the content of P4VP, P4VP patches aggregate into hydrophobic continuous phase and 'inverse hamburger' form (Scheme 3-3). When the amount of hydrophilic PEG chains was insufficient to stabilize the micelles, massive hydrophobic P4VP areas would be exposed on the surface of the micelles. MSPMs will transform into a transient morphology—Janus-type micelles (Scheme 3-4). Such Janus-type micelles cannot be stable in solution, which can serve as building subunits and self-assemble into various new equilibrium states (Scheme 3-5, 3-6 and 3-7). The morphology of these MMs depends on the number of subunits that participate in the assembling process.

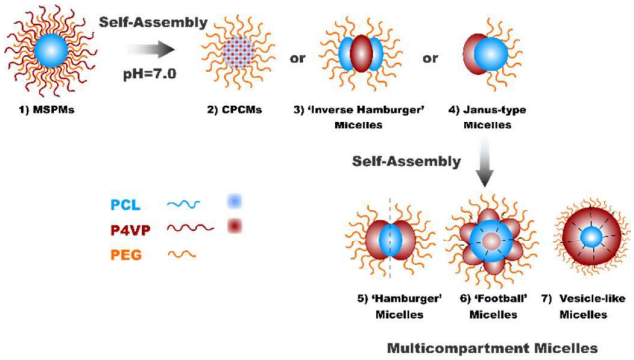

Scheme 3. Schematic representation of the forming process of the MMs.

Light scattering tests were applied to characterize the as-prepared MMs with different compositions. The results are presented in Figure 4 and Table 3. From the plot of D_t versus q^2 and the distribution of D_h, the translational diffusion coefficient D of the MMs are almost constants, which demonstrate the freshly-formed MMs with different compositions still keep spherical. The D_h of MMs is narrowly distributed, which confirms the homogeneity of the MMs. However, compared with the original MSPMs, the R_h of MMs increase obviously. The main reason for this is that the MMs can consist of several subunits, which enlarge their grain diameter. For the subunits with different compositions, along with the increase of their hydrophobic area, more subunits assembled together and formed a larger aggregation, which make the corresponding MMs exhibit an increasing grain diameter. At the same time, the increase in the assembling subunits make the structure of the MMs more incompact.

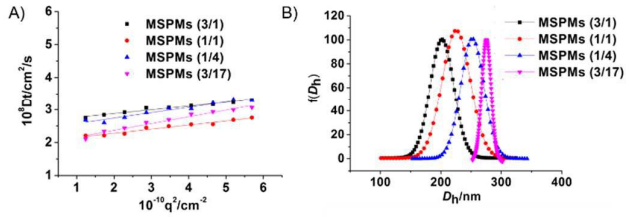

Figure 4. A) Angular dependence of the translational diffusion coefficient D_t and B) hydrodynamic diameter distribution f(D_h) of the MMs constructed by the subunits with four compositions of PEG-*b*-PCL/PCL-*b*-P4VP (pH=7.0, scattering angle=90 °).

Table 3. The R_g, R_h and R_g/R_h of the multicompartment micelles with four compositions of PEG-*b*-PCL/PCL-*b*-P4VP (pH=7.0).

Multicompartment Micelles (MMs) (PEG-*b*-PCL/PCL-*b*-P4VP)	R_g/nm	R_h ‡/nm	R_g/R_h
MMs (3/1)	74.1	92.8	0.798
MMs (1/1)	100.8	121.1	0.832
MMs (1/4)	111.9	131.8	0.849
MMs (3/17)	124.5	145.5	0.856

^{1}H NMR and 2D NOE spectra were used to further study MSPMs and their corresponding assembly--MMs. MSPMs (1/1) were taken as the observing object in D_2O under acidic condition, while MMs (1/1) could be formed through raising pH value in MSPMs solution. In Figure 5, peaks a (8.0-8.7) and b (7.1-7.6), due to P4VP blocks, are evident in the spectrum of MSPMs, which means that P4VP blocks on the surface of MSPMs are water soluble. On the contrary, for MMs, peaks owing to P4VP blocks disappear, indicating that P4VP blocks

turn hydrophobic and MSPMs transform into MMs. When two protons of chemically different monomers are in close proximity (distance<0.5 nm), cross peaks will be present in the 2D NMR spectrum.[34] Therefore, 2D NOE may provide valuable insights into MSPMs and MMs. Figure 6 shows the NOESY spectra of MSPMs (1/1) and MMs (1/1). Cross peaks could be observed at the intersection of the ^{1}H NMR signals of P4VP and PEG in the spectrum of MSPMs (Figure 6A), which confirms PEG and P4VP chains homogeneously mixed in the shell of MSPMs. However, the cross peaks are not observed in the spectrum of MMs (1/1) (Figure 6B), meaning that microphase separation occurs among PEG and P4VP chains and MMs come into being.

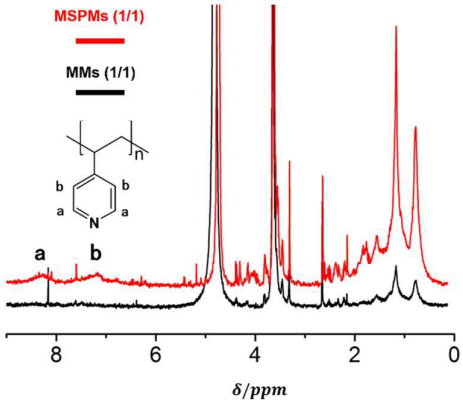

Figure 5. The ^{1}H NMR spectra of MSPMs (red line) and their corresponding assembly--MMs (black line).

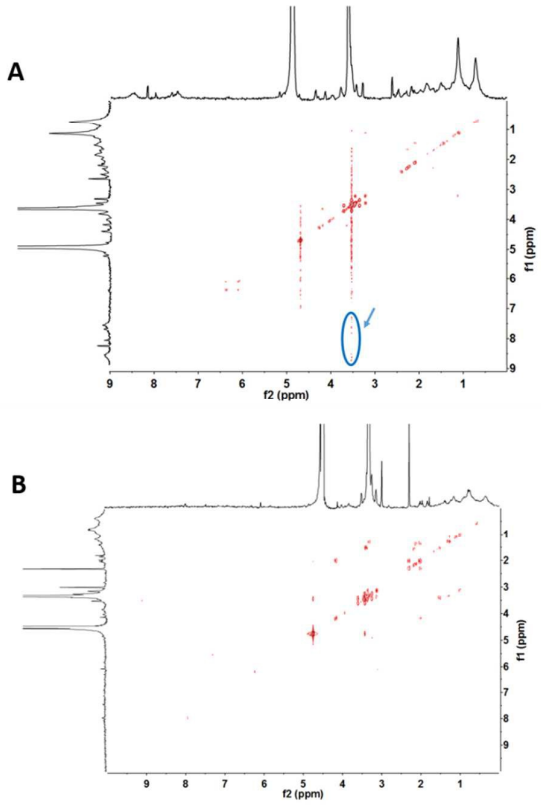

Figure 6. 2D NOE spectra of MSPMs (A) and MMs (B) in D_2O. Arrows indicate where cross peaks between P4VP and PEG should occur in case of close proximity.

Furthermore, TEM was applied to visualize the structure of the MMs. The details of the TEM samples can be enhanced by stains. Herein, uranyl-acetate, which can positively stain the P4VP chains of the MMs, was used to enhance the contrast of the various composition compartments in the MMs. In the TEM images, P4VP chains are stained by uranyl-acetate and show darker contrast. From these TEM images, MMs with different phase separation structures can be clearly observed. The morphology of these MMs is dependent on the composition of the subunits.

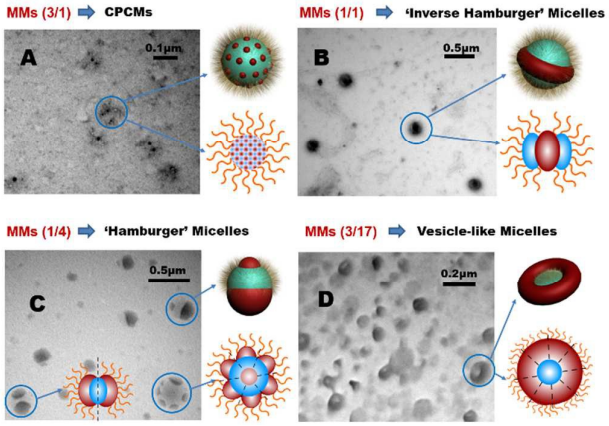

Figure 7. TEM images of the MMs constructed by the subunits with four compositions of PEG-*b*-PCL/PCL-*b*-P4VP (pH=7.0).

When P4VP chains are less, hydrophilic PEG chains can stabilize the micelles, and hydrophobic aggregation cannot occur among micelles themselves. In Figure 7A, stained hydrophobic P4VP chains aggregate as the dark patches spread around the surface of the MMs (3/1), indicating that MMs (3/1) are mainly CPCMs. The size of CPCMs is ca. 100 nm in the TEM image, which is smaller than that from the DLS results (200 nm). Both TEM image and DLS results show a uniform size distribution of CPCMs.

When P4VP contents further increase and the composition of the MSPMs reaches to 1/1, from the TEM image (Figure 7B), we can see that, the morphology of the MSPMs (1/1) transforms into 'inverse hamburger' micelles. So many hydrophobic P4VP patches aggregate that continuous P4VP Hydrophobic phase comes into being on the surface of the micelles. Such 'inverse hamburger' micelles can also further evolve and assemble under some conditions. For example, creating a non-solvent environment for PEG chains, 'inverse hamburger' might proceed colloidal polymerization and form worm-like 'colloidal polymers', which have appeared in some literatures.[35] However, in our system, PEG chains are still sufficient and hydrophilic to stabilize the micelles and prevent their aggregation. Therefore, only 'inverse hamburger' micelles can be observed. The resulted 'inverse hamburger' micelles possess a size of ca. 150 nm, which is a little smaller than that from DLS results (ca. 220 nm).

According to Müller's literature,[13] further increasing the hydrophobic P4VP components, the morphology of the MSPMs can transit into transient Janus-type micelles (scheme 3-4). Janus-type micelles have too many hydrophobic P4VP areas and less hydrophilic PEG chains so that they cannot be stable in solution anymore, which makes them difficult to be caught solely in solution. However, we find diverse hierarchical assembling morphologies by Janus-type micelles in Figure 7c, including 'hamburger' and 'football' micelles. 'Hamburger' micelles can be assembled by two subunits. When the assembling subunits appear in different sizes, the resulted hierarchical assembled morphology can be interesting 'pinecone' micelles—a kind of special 'hamburger' micelles. Multi-subunits can also assemble into 'football' micelles. Though TEM image presents various morphologies of MMs, their size distribution from DLS results (Figure 4B) is still relatively narrow, and the R_h we got is ca. 250 nm, which indicates that the MMs constructed by MSPMs (1/4) may focus on 'hamburger' micelles mainly.

Furthermore, when MSPMs (3/17) acted as the basic building subunits to construct MMs, the MMs with a completely fresh structure could be observed in the TEM images (Figure 7D). We speculate that this kind of structure of MMs might be vesicle-like, which is rarely observed in MMs system.[36] Under some conditions, amphiphilic copolymers with P4VP blocks can form vesicular structures. For example, the relatively short P4VP block biases the formation of bilayered structures in a selective solvent.[37] However, different from the vesicular structure in the literatures, the vesicular wall in our system seems thicker in the TEM image and their structure is also more compact from the R_g/R_h results in Table 3. The reason for this is probably that the building unit for our vesicle-like structure is Janus-type micelles, instead of direct macromolecular amphiphile in the literatures. The forming mechanism of such structure need further research and discussion.

Conclusions

Utilizing Müller's directed step-wise self-assembly method, we demonstrated the precise assembly of multicompartment micelles (MMs) based on two amphiphilic diblock copolymers for the first time. The directed step-wise self-assembly via pre-assembled subunits generate thermodynamically labile morphologies of MMs with extremely homogeneous structure. Moreover, compared with the previous tri-block copolymers system in Müller's method, diblock copolymers are more convenient to synthesize, and therefore the homogeneity as well as the dispersivity can be well controlled, which is beneficial for further assembly of the MMs. Beyond that, the structure and morphology regulation of MMs in our system is also very convenient, only through changing the composition ratio of these two diblock copolymers in the subunits. The resulting MMs exhibit control of the morphology, wherein the dimensions can be tailored to potentially suit for sensing applications or the patterning of surfaces via nanolithographic procedures. Making use of different hydrophobic compartments, including the hydrophobic core and hydrophobic patches, selective entrapment of dyes and drugs might be prone to realize in the near further.[38]

Acknowledgements

The work was financially supported by Natural Science Foundation of China (51403093, 51373073 and 51403149) and Natural Science Foundation of Zhejiang Province, China under Grant no.LQ13B070002.

Notes and references

[‡]We substitute R_h at the scattering angle of 90° for those obtained by angular extrapolation for simplification because all of the micellar systems involved in this study have monodisperse and narrow size distributions, no remarkable angular dependence of the translational diffusion coefficient D_t of these systems are observed in the scattering angle range of 35°-135°, i.e., R_h calculated from D_t by the Stokes-Einstein equation do not have a remarkable angular dependence.

1 G. M. Whitesides, J. P. Mathias and C. T. Seto, *Science*, 1991, **254**, 1312.
2 G. M. Whitesides and B. Grzybowski, *Science*, 2002, **295**, 2418.
3 M. Lazzari and M. A. Lopez-Quintela, *Adv. Mater.*, 2003, **15**, 1583.

4 S. Foster and M. Antonietti, *Adv. Mater*., 1998, **10**, 195.
5 F. Schacher, E. Betthausen, A. Walther, H. Schmalz, D. V. Pergushov and A. H. E. Müller, *ACS nano*, 2009, **3**, 2095.
6 K. Kataoka, A. Harada and Y. Nagasaki, *Adv. Drug Delivery Rev*., 2001, **47**, 113.
7 K. Yoshimatsu, B. K. Lesel, Y. Yonamine, J. M. Beierle, Y. Hoshino and K. J. Shea, *Angew. Chem. Int. Ed*., 2012, **51**, 2405.
8 X. Wang, G. Guerin, H. Wang, Y. Wang, I. Manners and M. A. Winnik, *Science*, 2007, **317**, 644.
9 X. M. He and D. C. Carter, *Nature*, 1992, **358**, 209.
10 A. Laschewsky, *Curr. Opin. Colloid Interface Sci*., 2003, **8**, 274.
11 S. Park, J. -H. Lim, S. -W. Chung and C. A. Mirkin, *Science*, 2004, **303**, 348.
12 D. J. Hill, M. J. Mio, R. B. Prince, T. S. Hughes and J. S. Moore, *Chem. Rev*., 2001, **101**, 3893.
13 A. H. Gröschel, F. H. Schacher, H. Schmalz, O. V. Borisov, E. B. Zhulina, A. Walther and A. H. E. Müller, *Nat. Commun*., 2012, **3**, 710.
14 A. H. Gröschel, A. Walther, T. I. Löbling, J. Schmelz, A. Hanisch, H. Schmalz and A. H. E. Müller, *J. Am. Chem. Soc*., 2012, **134**, 13850.
15 A. H. Gröschel, A. Walther, T. I. Löbling, F. H. Schacher, H. Schmalz and A. H. E. Müller, *Nature* 2013, **503**, 247.
16 B. Fang, A. Walther, A. Wolf, Y. Xu, J. Yuan and A. H. E. Müller, *Angew. Chem. Int. Ed*., 2009, **48**, 2877.
17 I. K. Voets, A. de Keizer and M. A. C. Stuart, *Adv. Colloid Interface Sci*., 2009, **147-148**, 300.
18 C. L. Wu, R. J. Ma, H. He, L. Z. Zhao, H. J. Gao, Y. L. An and L. Q. Shi, *Macromol. Biosci*., 2009, **9**, 1185.
19 A. B. E. Attia, Z. Y. Ong, J. L. Hedrick, P. P. Lee, P. L. R. Ee, P. T. Hammond and Y. Y. Yang, *Curr. Opin. Colloid Interface Sci*., 2011, **16**, 182.
20 J. P. Lin, J. Q. Zhu, T. Chen, S. L. Lin, C. H. Cai, L. S. Zhang, Y. Zhuang and X. S. Wang, *Biomaterials*, 2009, **30**, 108.
21 S. V. Vinogradov, E. V. Batrakova, S. Li and A. V. Kabanov, *Drug Targeting*, 2004, **12**, 517.
22 R. Zheng, G. Liu and X. Yan, *J. Am. Chem. Soc*., 2005, **127**, 15358.
23 Z. Li, M. A. Hillmyer and T. P. Lodge, *Macromolecules*, 2006, **39**, 765.
24 M. J. Barthel, A. C. Rinkenauer, M. Wagner, U. Mansfeld, S. Hoeppener,; J. A. Czaplewska, M. Gottschaldt, A. Träger, F. H. Schacher and U. S. Schubert, *Biomacromolecules*, 2014, **15**, 2426.
25 S. N. Sidorov, L. M. Bronstein, Y. A. Kabachii, P. M. Valetsky, P. L. Soo and D. Maysinger, *Langmuir*, 2004, **20**, 3543.
26 K. N. Jayachandran, A. Takacs-Cox and D. E. Brooks, *Macromolecules*, 2002, **35**, 4247.
27 M. Ciampolini and N. Nardi, *Inorg. Chem*., 1966, **5**, 41.
28 J. H. Xia, X. Zhang and K. Matyjaszew ski, *Macromolecules*, 1999, **32**, 3531.
29 W. van Zoelen, G. A. van Ekenstein, O. Ikkala and G. ten Brinke, *Macromolecules*, 2006, **39**, 6574.
30 T. R. Hui, D. Y. Chen and M. Jiang, *Macromolecules*, 2005, **38**, 5834.
31 X. Liu, R. Ma, J. Shen, Y. Xu, Y. An and L. Shi, *Biomacromolecules*, 2012, **13**, 1307.
32 C. Wu, J. Zuo and B. Chu, *Macromolecules*, 1989, **22**, 633.
33 J. F. Gohy, S. K. Varshney, S. Antoun and R. Jérôme, *Macromolecules*, 2000, **33**, 9298.
34 C. Wu, R. Ma, H. He, Li, Zhao, H. Gao, Y. An and L. Shi, *Macromol. Biosci.*, 2009, **9**, 1185.
35 A. H. Gröschel and A. H. E. Müller, *Nanoscale*, 2015, **7**, 11841.
36 W. Zhao, D. Chen, Y. Hu, G. M. Grason and T. P. Russell, *ACS nano*, 2011, **5**, 486.
37 D. Chen, S. Park, J. T. Chen, E. Redston and T. P. Russell, *ACS Nano*, 2009, **3**, 2827.
38 J. -F. Lutz and A. Laschewsky, *Macromol. Chem. Phys.,* 2005, **206**, 813.

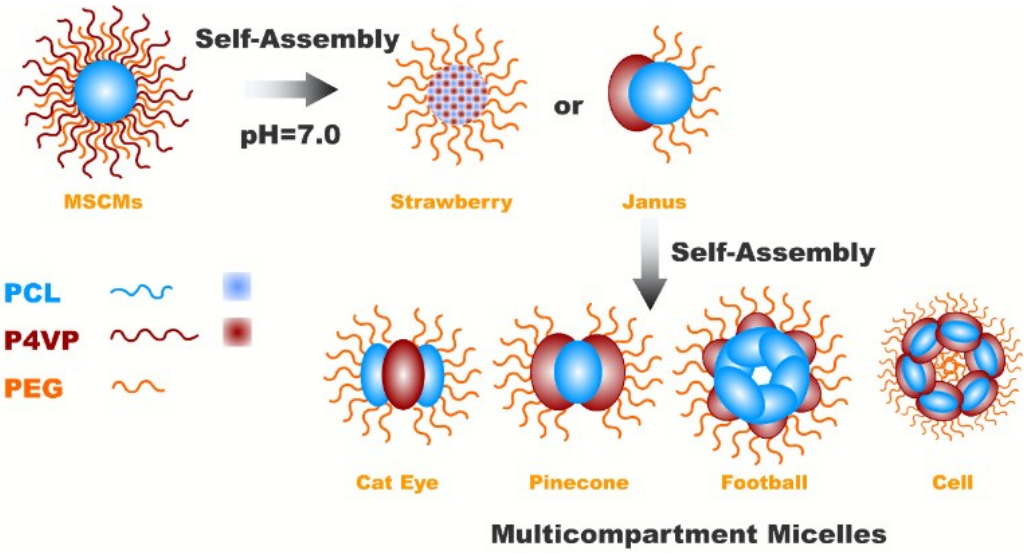

Multicompartment micelles with various morphologies are prepared via a directed step-wise self-assembly using pre-assembled subunits. The pre-assembled subunits are first constructed through the co-assembly of two amphiphilic diblock copolymer, including PCL-*b*-PEG and PCL-*b*-P4VP.

.